MAUSAM, **69**, 1 (January 2018), 1-18

551.501.8 : 551.553.21 (267.64)

Differential patterns of surface winds over Bay of Bengal during the various phases of Indian northeast monsoon derived from QuikSCAT data, 1999-2008

B. AMUDHA, Y. E. A. RAJ and RM. A. N. RAMANATHAN

Regional Meteorological Centre, India Meteorological Department, Chennai – 600 006, India

(*Received 29 November 2016, Accepted 1 November 2017*)

e mail : amudha2308@gmail.com

सार – 1999-2008, दस वर्षों की अवधि के भारतीय उत्तर पूर्वी मानसून मौसम अक्तूबर-नवम्बर-दिसम्बर के विभिन्न फेस के दौरान सतही हवाओं के अवकलित पैटर्न का विश्लेषण क्विक स्केटोमीटर का प्रयोग करके किया गया है, जैसे 77 से 100° और 0 से 25° से घिरे बंगाल की खाड़ी के ऊपर के क्षेत्र में 0.25 × 0.25° विभेदन पर सागर की सतही हवा पर आधारित क्विक स्कैट। उत्तर पूर्वी मानसून के आरंभ के समय पर अक्तूबर में 14° के लगभग अक्तूबर-नवम्बर-दिसम्बर के दौरान सागरीय सतही हवाओं के वायु सदिस और अदिस वायु गति का पॉच दिन के औसत से विषवत् द्रोणी के स्थापित होने की पुष्टि हुई और इसके तत्पश्चात वापसी के दौरान दिसम्बर तक 2 से 3° उत्तर में चला जाता है। उत्तर पूर्वी मानसून के आरम्भ से पहले और विषवत् द्रोणी के दक्षिण की तरफ आगे बढ़ने के बाद आरम्भ से पूर्वी हवाओं के विसरण की प्रकृति से निकलने वाली आरम्भ की तारीखों पर आधारित तीन दिन की घटना को अध्यारोपित करके विशलेषण किया गया है।

उत्तर पूर्वी मानसून के पॉच फेस के दौरान हवा के पैटर्न का औसत जैसे उत्तर पूर्वी मानसून से पहले (C_1), क्रियात्मक (C_2), हलके (C_3), शुष्क (C_4) और जमीन के ऊपर आर एफ क्रिया-क्लापों के आधार पर उत्तर पूर्वी मानसून के वापसी (C_5) के दिनों के बाद को वर्गीकृत करके उत्पादित किया गया था जिससे C_2 में लगभग 6° उत्तर से C_5 के दौरान 2 से 3° उत्तर में विषवत् द्रोणी के दक्षिण की तरफ गति को दिखाता है। C_2 से C_5 तक बंगाल की खाड़ी के मन्नार की खाड़ी और कोमोरिन क्षेत्रों के ऊपर उत्तरी हवाएँ 8-9 मीटर प्रति सैकिंड की गति के साथ चलती रहती है। बंगाल की खाड़ी के पॉच उल्लेखित क्षेत्रों में क्विक स्केटरोमीटर हवाओं के औसत बहिर्गमन दीर्घतरंग विकिरण (ओ एल आर) O_1 से O_4 (तीव्र से संवहन की अनुपस्थिति) के चार वर्गो के तहत उत्तरपूर्वी मानसून के दिनों के समूह तैयार किये जाने से बंगाल की खाड़ी के ऊपर अधिकांशतः पूर्वी (O_1) से उत्तरपूर्वी होना (O_2, O_3) और उत्तरी हो जाती है। C_2 और O_1 दिनों के दौरान तमिलनाडु तट के नजदीक हवा की गति पूर्व से उत्तर 7-9 मीटर प्रति सैकिंड तक पहुँच जाती है जबकि दूसरे फेस के दौरान बंगाल की खाड़ी के मुहाने पर हवा की गति उत्तर से दक्षिण बढ़ती है पर पॉच मीटर प्रति सैकिंड से कम रहती है। पॉच क्षेत्रों में अदिस वायु गति (मी./सै.) का औसत O_1 में (7.8) अधिकतम और O_4 दिनों में सबसे कम (6.2)। क्विक स्केटरोमीटर वायु गति 10 मी. ऊँचाई के संदर्भ की अपेक्षा बॉय से प्राप्त ऑकड़ों से प्राप्त वायु गति माध्य समुद्र स्तर से 11 प्रतिशत कम है जिसे उर्ध्वाधर पर एम.एस.एल. से 3 मीटर की दूरी में हवाओं की लधुगुणांक अस्थिरता के सैद्धान्तिक अवधारणा का प्रयोग करके निर्धारित किया गया है। हवा की गति क्विक स्केटरोमीटर और बॉय दोंनों अच्छें तुलनात्मक है यदि समान संदर्भ सतर से लिया गया हो।

ABSTRACT. The differential patterns of surface winds during the various phases of the Indian northeast monsoon (NEM) season October-November-December (OND) of the 10 year period 1999-2008 have been analysed using Quick Scatterometer (QS) *viz*., QuikSCAT based ocean surface wind (OSW) data at 0.25° × 0.25° resolution in the region bounded by 77- 100° E and 0-25° N over Bay of Bengal (BoB). The pentad mean wind vector (WV) and scalar wind speed (WS) of OSW during OND revealed firm establishment of Equatorial Trough (ET) along 14° N in October at the time of onset of NEM and its subsequent shift to 2-3° N by December during withdrawal. Triad superposed epoch analysis based on onset dates brought out the diffused nature of easterly winds prior to onset and the southward movement of ET after onset.

Mean wind patterns during the five phases of NEM *viz*., pre-NEM (C_1), active (C_2), light (C_3), dry (C_4) and post-NEM withdrawal (C_5) days classified based on RF activity over land were generated which showed the southward movement of the ET from around 6° N in C_2 to 2-3° N during C_5. Northerly winds with WS of 8-9 m/s prevailed over Gulf of Mannar (GoM) and Comorin areas of BoB throughout C_2 to C_5. The mean QS winds in five defined sectors of BoB derived by grouping the days of NEM under four categories of outgoing longwave radiation (OLR) O_1 to O_4 (intense to no convection) revealed prevalence of easterlies (O_1) becoming northeasterlies (O_2, O_3) and northerlies (O_4) over most of BoB. During C_2 and O_1 days, WS increases from east to west reaching 7-9 m/s close to Tamil Nadu coast while during other phases, WS increases from north to south with WS less than 5 m/s over head BoB. Over the five sectors, mean scalar WS (m/s) is highest (7.8) in O_1 and least (6.2) in O_4 days. The buoy measured WS at 3 m from m.s.l.

is lower by 11% than the QS WS referenced to 10 m height as determined using the theoretical concept of logarithmic variability in winds over the vertical. WS from both QS and buoy are well comparable when brought to the same reference level.

Key words – Bay of Bengal, Buoy, Equatorial trough, Northeast monsoon, Outgoing longwave radiation, Ocean surface winds, QuikSCAT, Superposed epoch analysis.

1. Introduction

The Indian Northeast Monsoon (NEM) is a small scale winter monsoon confined to parts of South Peninsular India (SPI) with duration from 1 October to 31 December. It sets in by early October after the withdrawal of Southwest Monsoon (SWM) from most parts of India and retreats by the end of December. The NEM rainfall (RF) characteristics over SPI have been widely researched, few being Raj and Jamadar (1990); Raj (1992, 2003, 2012); Geetha (2011) and Geetha and Raj (2015). India Meteorological Department (IMD) defines monsoon activity over land based on RF realised, whereas over oceans, the strength of the monsoon is defined based on the speed of ocean surface winds (OSW). For the Indian NEM benefitting SPI, the major source of moisture feed is the adjoining Bay of Bengal (BoB) which is part of North Indian Ocean (NIO). Monitoring the variations in OSW over BoB hence becomes a crucial factor in observing the performance of the Indian NEM itself.

Historically, sailors visually estimated OSW based on the appearance of the surface of the sea and recorded them in ships' log books, a practice which dates back to the 17th century. In recent years, near real time OSW data is available from moored / drifting data buoys deployed over the oceans and fitted with sensors for measurement of meteorological parameters including wind vector (WV) *i.e.*, wind direction (WD) and wind speed (WS) over the surface of oceans. Advances in remote sensing technology paved the way for mapping the OSW profile at different levels of the atmosphere on real or near-real time basis. The Indian geostationary satellites Kalpana-1 (September 2002), INSAT-3A (April 2003) and INSAT-3D (July 2013) provide cloud motion vectors as derived products, which indicate the flow pattern of winds at 850 (1.5 km), 700 (3.1 km) and 500 hPa (5 km) pressure levels but not at the surface level over land/ocean.

Even prior to the 1980s, remote sensed wind data from the upper levels of the atmosphere other than the surface level was available. In 1973, the launch of a space-borne satellite Skylab with onboard synthetic aperture kind of radar microwave instrumentation capable of mapping OSW was a major technological breakthrough. OSW data was available from subsequent missions *viz.*, Seasat (1978), Nimbus-7 (1978-1994), SSM/I (1987), ERS-I & II (1991, 1995), NSCAT (1996), SeaWinds on QuikSCAT (Quick Scatterometer, QS, 1999), SeaWinds on ADEOS-2(2002) and ASCAT (ESA / EUMETSAT, 2006). OSW derived from QS data are available at a high grid resolution of up to 0.25° × 0.25°. QS data has been utilised by researchers to understand characteristic features of OSW [Liu (2002); Sarkar (2003); Loe *et al.* (2006); Agarwal *et al.* (2007); Satheesan *et al.* (2007) and Singh and Singh (2011)]. In the present study, the high resolution OSW over BoB, available from QS has been utilised to derive wind patterns associated with the various episodes of NEM over land and ocean.

The scope and objectives of the study are listed below:

(*i*) To generate and analyse the mean QS based OSW over BoB of days grouped under five day periods (pentads) of the NEM season for the period 1 October - 31 December, 1999-2008 (10 years).

(*ii*) To perform superposed epoch analysis on the OSW data with reference to onset dates of NEM and generate mean spatial patterns of winds for various triads.

(*iii*) To derive and bring out the spatial patterns of the mean OSW during various phases of the NEM activity over land.

(*iv*) To determine the mean OSW over five sectors of BoB which influence NEM by classifying the days among four defined categories of outgoing longwave radiation (OLR) excluding days of cyclonic disturbances (CDs).

(*v*) To perform a similar analysis using the OSW data from moored buoys for the different phases of NEM activity over land.

(*vi*) To undertake a theoretical comparison of the variability between QS OSW at 10 m and buoy based winds at 3 m height above mean sea level (m.s.l.).

2. Area of study

The region bounded by 77-100° E and 0-25° N which includes BoB and parts of NIO is the area of study as depicted in Fig. 1 over which the QS derived OSW data are analysed. To issue cyclone warnings and coastal weather bulletins, IMD has divided BoB into six sections (IMD, 2003), out of which west central (WC, 13°-18.5° N,

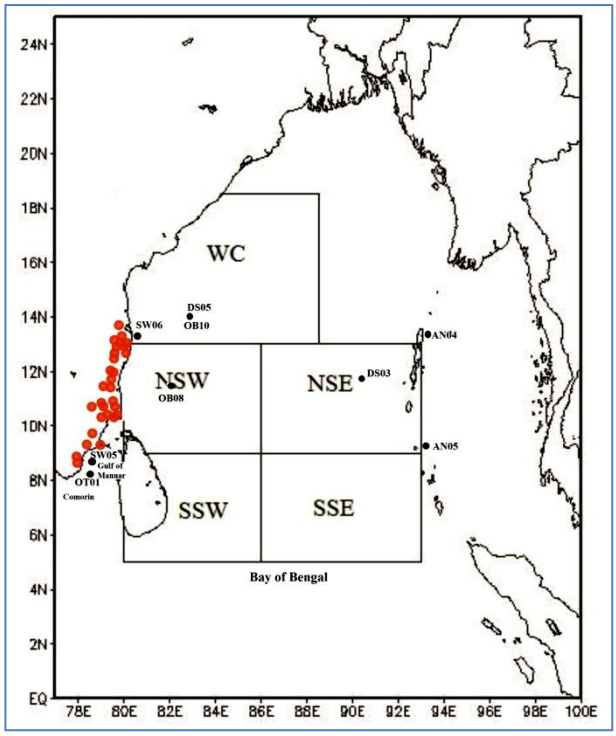

Fig. 1. Five demarcated sectors of BoB in the area of study. Locations of 9 moored buoys and 29 rain gauge stations of CTN and SCAP are also shown.
(WC : West Central, NSW : North South West, NSE : North South East, SSW: South South West, SSE: South South East)

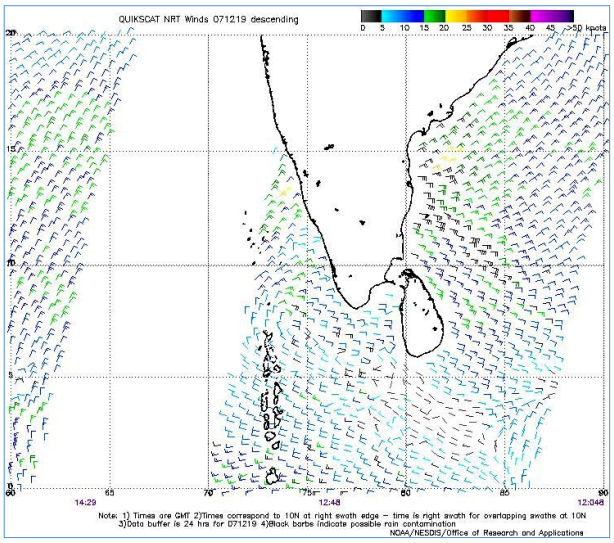

Fig. 2. Sample image of a descending pass on 19th December, 2007 displaying OSW from QS
Note : Wind direction (in degrees) and wind speed (in knots) are as per meteorological convention

80°-88.5° E), southwest (SW, 5°-13° N, 80°-86° E) and southeast (SE, 5°-13° N, 86°-93° E) are of particular interest. For this study, both SW and SE BoB are further sub-divided into two parts each *viz*., north SW BoB (NSW, 9°-13° N, 80°-86° E) and south southwest (SSW, 5°-9° N, 80°-86° E), north SE (NSE, 9°-13° N, 86°-93° E) and south SE (SSE, 5°-9° N, 86°-93° E). The geographical extent of the five sectors of BoB thus considered is also depicted in Fig. 1.

3. Technical details of QuikSCAT and moored buoys

In this section, a few technical and instrumental details of QS and moored buoys are presented. The scope and type of data available as relevant to the present study are discussed.

3.1. *Quick scatterometer*

The QS was launched by the National Aeronautics and Space Administration on 19 June, 1999 and its functionality ended on 23 November, 2009. The QS has a special active microwave radar using Ku-band with an operating frequency of 13.4 GHz and a nominal sun-synchronous circular orbit. The QS orbit ascending and descending equator crossings are at local times of 6 am and 6 pm respectively. QS located at an altitude of 803 km above m.s.l. over the equator had a continuous 1800 km swath covering 93% of the global ocean in a single day. Orbital period was 101 minutes at 14.25 orbits per day (PODAAC, 2001).

The Sea winds instrument onboard the QS satellite is an active microwave scatterometer which transmits radar pulses and measures the backscattered energy returned to the satellite due to waves or ripples on the ocean surface. Modulation of the waves due to wind alters the surface roughness of the ocean and hence the magnitude of the backscattered power affecting the normalised radar cross section (σ_o) of the ocean surface. A rough (smooth) ocean surface returns a stronger (weaker) signal because the waves reflect more (less) of the radar energy back toward the QS antenna. Hence σ_o is empirically related to wind through a geophysical model function. The equivalent neutral winds (Liu and Tang, 1996) computed for a reference height of 10 m above m.s.l. are considered as OSW (QS manual, 2006).

In QS data processing, measurements close to land are excluded to eliminate land contamination resulting in a data gap within 25 km from the shore-line (Wenqing *et al*., 2004). During rains, σ_o gets contaminated as some of the transmitted energy scattered and / or absorbed by the rain is not measured by the scatterometer. Rain flagging techniques have been used in the algorithm for detection and removal of rain contaminated OSW. The scrutiny of

the images of QS passes indicated that such flagged contaminated data had been removed to a large extent in the text data containing the zonal *(u)* and meridional (*v)* components of the ascending and descending passes.

3.2. *Moored buoys deployed over Bay of Bengal*

In situ meteorological observations over NIO are available from the moored data buoys equipped with GPS and satellite trans-receivers and deployed at specific Long./ Lat. coordinates by National Institute of Ocean Technology (NIOT) Chennai since 1997. The wind sensor (either mechanical or ultrasonic) is mounted at a height of approximately 3 m above m.s.l. (Venkatesan *et al.*, 2013). The data is available both on real time basis and in archived form through Indian National Centre for Ocean Information Services (INCOIS), Hyderabad.

4. Data

4.1. The QS Level-3 microwave radar gridded data files of the *u* and *v* wind components in text format for the daily ascending and descending passes were downloaded (http://opendap.jpl.nasa.gov/opendap/OceanWinds/quikscat/L3/jpl/v2/hdf/) for each day of the NEM season 1 October-31 December for the 10 year period 1999-2008. A sample QS image of the OSW mapped over BoB is presented in Fig. 2.

The QS OSW data at a high spatial resolution of 0.25° × 0.25° is available in the web site mentioned above, on a global grid of 1440 pixels in longitude (*x* grid, 0.125° to 359.875°, 360 × 4 = 1440) by 720 pixels in latitude (*y* grid, -89.875° to +89.875° South to North, 180 × 4 = 720). The total number of data files downloaded and processed was 1840 each for *u* and *v* respectively (*u*: 92 days × 10 years × 2 passes / day; Similarly, for *v*). Though ideally, *u* and *v* must be available from each pass over a grid point every day, the actual number of *u* and *v* values obtained is variable each day due to the changing swath area of the pass. During the period of study, data of 21 passes was completely missing. As such, over the area bounded by 77-100° E and 0-25° N considered for the study containing 93 × 101 = 9393 grid values per pass data, 1819 files each for *u* and *v* were available for processing. Three-fourth of the area of study *i.e.*, around 7000 grid points are over the oceanic areas and the remaining over land for which QS data is unavailable. Thus, overall, nearly 7000 grid values of *u* and *v* data each, per pass are available. In this way, approximately 28,000 grid point values of *u* and *v* per day over the oceanic study area were processed for further analysis.

4.2. The date of onset (DO) and date of withdrawal (DW) of NEM over CTN for the 10 year period 1999-2008 were utilised and are presented in Table 1.

TABLE 1

Dates of onset and withdrawal of Indian NEM, 1999-2008

Year	Onset	Withdrawal
1999-2000	04 O	12 J
2000-01	03 N	02 J
2001-02	15 O	01 J
2002-03	09 O	12 D
2003-04	19 O	08 D
2004-05	18 O	16 D
2005-06	11 O	21 D
2006-07	17 O	14 D
2007-08	19 O	07 J
2008-09	12 O	21 D
Mean	16 O	23 D
Normal (1901-2000)	20 O	30 D

NEM : Northeast Monsoon, O: Oct, N: Nov, D: Dec, J : Jan

4.3. Daily rainfall (DRF) data from 1 October to 31 December, 1999-2008 for 27 stations of CTN and 2 of south coastal Andhra Pradesh (SCAP) were collected from the records available at Regional Meteorological Centre (RMC), Chennai. The geographical locations of the stations along with those of Gulf of Mannar (GoM) and Comorin areas of BoB are provided in Fig. 1.

4.4. The daily temporal mean OLR data in text format for the period from 1 October to 31 December, 1999-2008 over the area of study was obtained from National Data Centre, IMD, Pune and the Satellite Meteorology Division, IMD, New Delhi. The grid resolution of OLR data used is 2.5° × 2.5° Long. / Lat. for 1999 and 1° × 1° for 2000-2008.

4.5. OSW data of 9 moored buoys deployed at specific Long. / Lat. coordinates over BoB by NIOT, Chennai was obtained from the archives of INCOIS, Hyderabad for the NEM season of 1999-2008. The time sampling of the WD and WS data ranged from hourly to three hourly for each buoy and so irrespective of the time interval, the data has been considered for computations. The locations of the 9 buoys are provided in Fig. 1.

5. Classification of convective activity based on OLR criteria

The rainfall distribution for a given day over 29 rain gauge stations (Fig. 1) of CTN and SCAP which are considered as representative of NEM activity gives an indication of the strength of NEM over SPI.

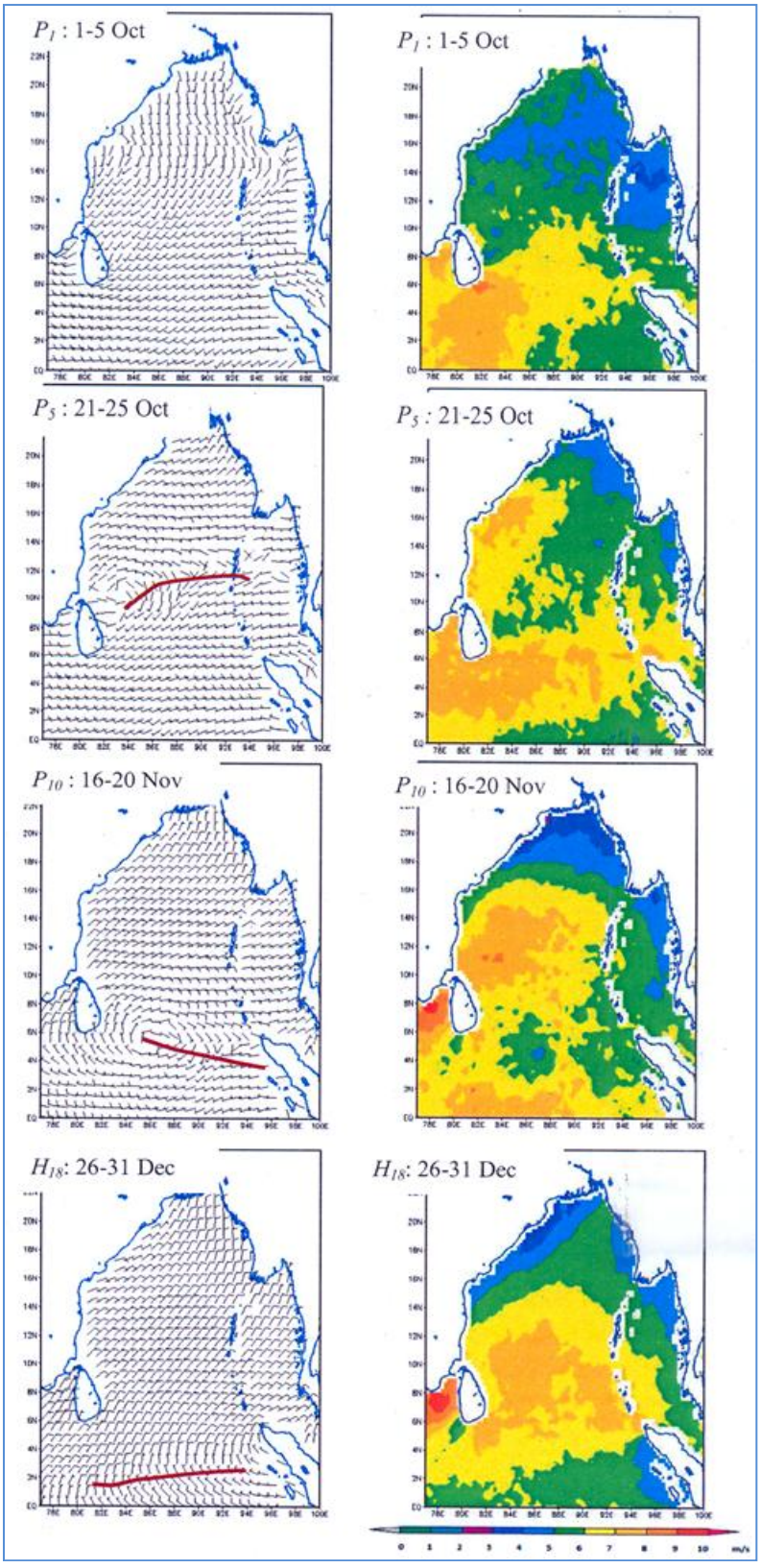

Fig. 3(a). QS mean OSW and mean scalar WS (in m/s) over BoB during NEM season, 1999-2008
P: Pentad, H: Hexad , OSW - Wind direction (in degrees) and wind speed (in knots) Trough line :

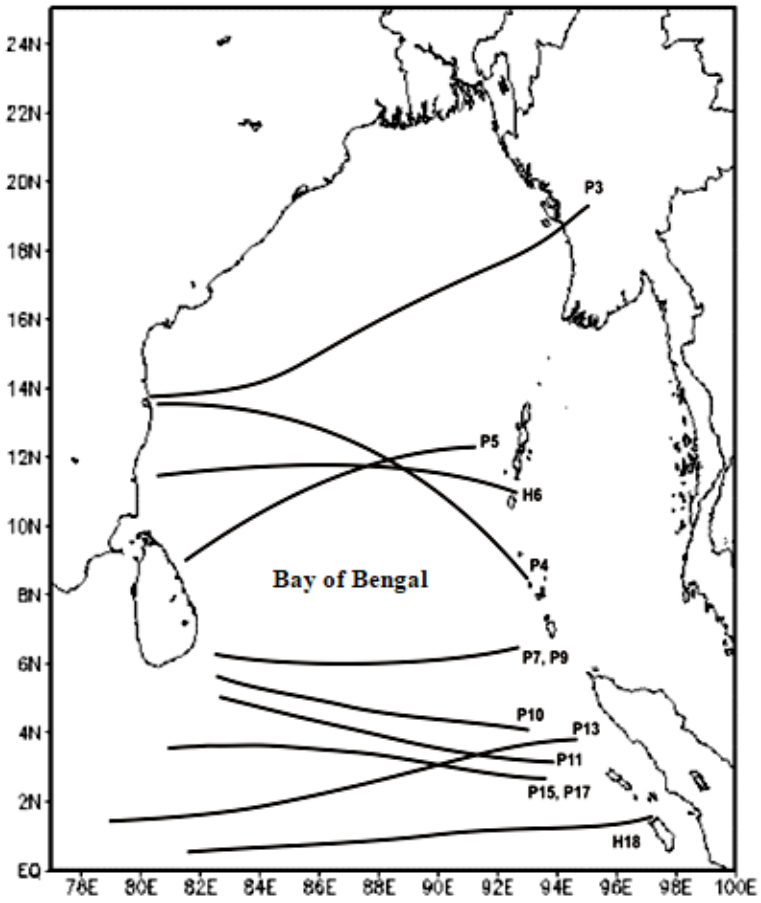

Fig. 3(b). Normal movement of surface equatorial trough over BoB based on pentad / hexad (P1-H18) analysis of QS OSW during NEM season, 1999-2008

Over the oceans, such an evaluation could potentially be done using satellite-derived OLR data. For the Indian region and adjoining BoB areas, utility of OLR data as a proxy indicator for clouding associated with NEM season has been established by Suresh and Raj (2001), Raj *et al.* (2007) and reiterated by Amudha *et al.* (2016a). For the Indian SWM, lower values of OLR in the range 200-220 Wm^{-2} are taken as indicative of typical monsoon clouding (IMD, 2008). However, for NEM, a higher but optimal threshold value of OLR230 ($OLR \leq 230 Wm^{-2}$) was used by Raj *et al.* (loc.cit.) to delineate and represent clouding associated with NEM over BoB and SPI due to the reason that NEM clouds are much shallower than SWM clouds. The same OLR threshold has been used in this study also. Further, four OLR based criteria to categorise days of convection are defined as follows: Very Intense / Intense Convection (O_1, $OLR \leq 200$ Wm^{-2}), Moderate (O_2, OLR 200-230 Wm^{-2}), Weak (O_3, OLR 230-240 Wm^{-2}) and cloud free or No Convection (O_4, OLR > 240 Wm^{-2}).

6. Methodology, analysis and results

6.1. *QuikSCAT based analysis*

6.1.1. *Pentad / hexad means*

For a given year, the duration of NEM season *viz*., 1 October-31 December was sub-divided into 16 pentads and 2 hexads (5 and 6 day periods respectively) indicated by P_1 (1-5 Oct), P_2 (6-10 Oct),…,H_6 (26-31 Oct), P_7, P_8,…,P_{17} and H_{18} (26-31 Dec). The values of u and v components as stated in Section 4.1 yield approximately 14,000 WVs per day over the oceanic area of study. The mean WVs at specific grid points for each pentad (hexad) for the 10 year period 1999-2008 were computed using 7 (8.4) lakhs gridded value data. The mean scalar WS at the grid points was also computed as it gives an indication of the strength of winds over the ocean surface. The generation of mean WV pattern provides an understanding of the movement of the large scale winds and hence the Equatorial Trough (ET) over

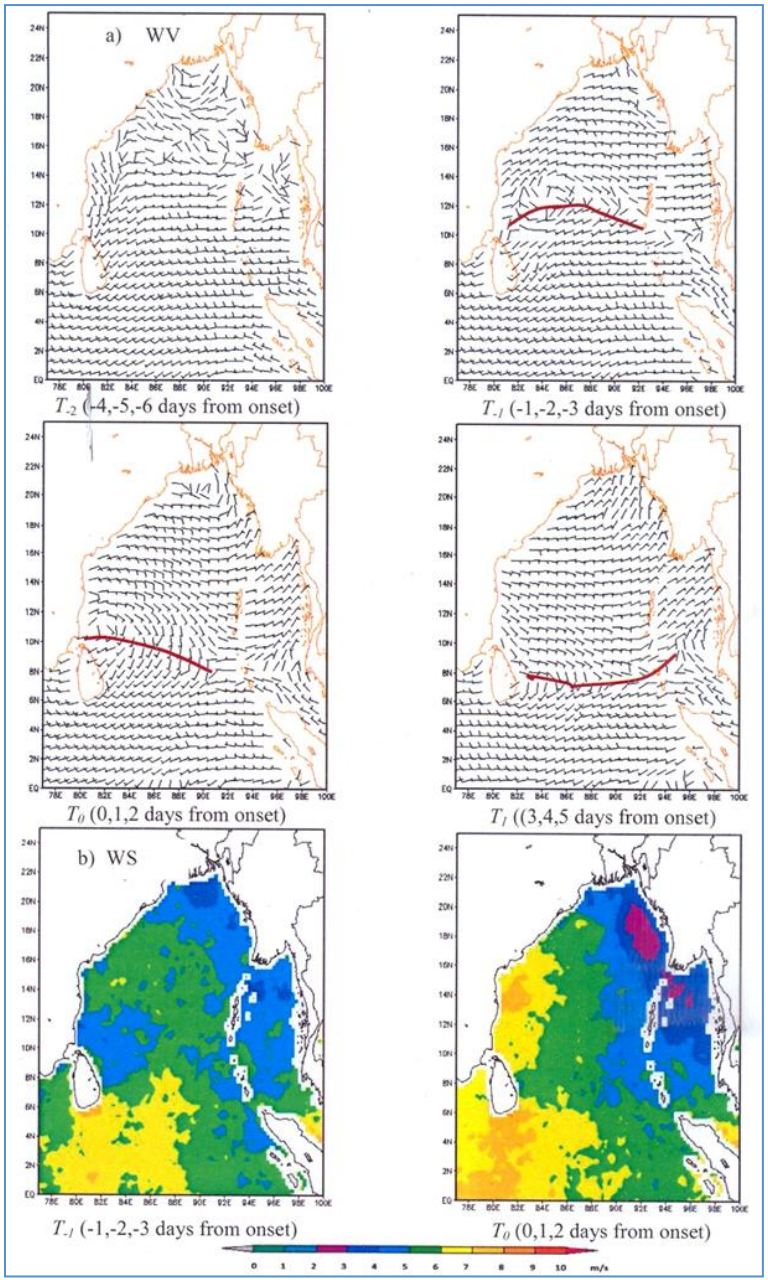

Figs. 4(a&b). QS mean OSW over BoB for a few triads based on NEM onset dates, 1999-2008
(a) WV - wind vector and (b) WS - scalar wind speed (in m/s)

BoB during the NEM season. The processes of evaporation of sea water and increase in moisture content over the sea are dependent on the magnitude or strength of the scalar winds over BoB which substantially differ from the vector WS. The pictorial spatial mean WV patterns and mean scalar WS (in m/s) patterns were generated for all pentads / hexads but only those of P_1, P_5, P_{10} and H_{18} which by and large are representative of the winds during the NEM season have been provided in Fig. 3(a). In all further similar pictorial depictions of WV by wind barbs in this study, the vector WS is in knots as per meteorological convention. The surface ET over BoB could be clearly delineated from the mean OSW pattern associated with pentads / hexads P_3 or after. The positions of the ET from P_3 to H_{18} save for P_8 and P_{12} which overlapped with pentads P_7 and P_{11} respectively are depicted in Fig. 3(b).

The salient features of the mean OSW pattern over BoB during NEM season observed from the analysis of all the pentads and those depicted in Fig. 3(a) and the ET positions displayed in Fig. 3(b) are discussed below:

During the pentads P_1 and P_2, SW winds dominating in lower latitudes become southerlies in higher latitudes. The transition of winds from southerlies to northeasterlies (NE) over north BoB as a prelude to the onset of NEM could be observed in P_3. Appearance of easterlies over extreme north BoB and the demarcation of easterly-westerly (E-W) winds with the firm establishment of the ET along 14° N [Fig. 3(b)] were clear from P_4. Movement of easterlies further southward with the onset of NEM and a prominent shift in the western (eastern) end of ET to 9 (12)° N is evident from P_5. In P_7 the ET further shifted southwards to 7° N near Sri Lankan land mass. In P_{10} (16-20 Nov) the western end of the ET is at 6°N while the eastern end is located around 4° N. In P_{13} (1-5 Dec) ET shifted closer to 2° N over western parts and to 5° N over eastern parts of south BoB. In H_{18}, ET is located close to 1.5° N.

The scalar WS patterns of P_1 depicted in Fig. 3(a) indicate that south of 8° N, WS of 6-8 m/s are observed in GoM and Comorin areas and the oceanic region south of Sri Lankan land mass has pockets of WS 8-9 m/s. North of 8° N, WS decreases from 5-6 m/s reaching 4-5 m/s north of 15° N and most parts of head BoB. In P_5, just after the normal onset of NEM, the strengthening of WS to 6-8 m/s in sectors of BoB close to CTN and SCAP, areas of GoM, Comorin and oceanic areas further south is evident. In P_{10}, pockets of WS 9-10 m/s are observed in Comorin area with a gradual decrease in WS from 7-8 m/s over central parts of BoB to 3-4 m/s over head BoB. During the hexad H_{18} which is the last sub-period of December when NEM has almost withdrawn from CTN, a strong WS pocket of 9-10 m/s prevails over GoM and Comorin areas. A large sector over central parts of BoB south of 13° N experiences WS of 8-9 m/s. The ET is by and large oriented E-W and moves from north to south as the season advances. In the case of P_4 , the eastern end of ET dips to a much more southerly latitude of 9° N compared to the western end which is at 14° N. The ETs of P_7 and after, are all located south of 6° N and that of H_{18} close to the equator.

6.1.2. *Triad variability of QS winds based on superposed epoch analysis*

The compositing technique known as superposed epoch analysis (Panofsky & Brier, 1968) was used to derive the spatial and temporal distributions of QS winds for 6 triads prior to and after the onset of NEM. The DO of each year (Table 1) is considered as the '0^{th}' day and the calendar dates preceding DO are assigned as -1, -2, -3…and succeeding dates as 1, 2, 3,…. The QS winds for a triad, for a given grid point is the average of winds for the 3 days. Thus, WVs of -7,-8 and -9 days are averaged to derive the WV of -3 triad (T_{-3}). Similar grouping is done for T_{-2} (-4, -5, -6), T_{-1} (-1, -2, -3), T_0 (0, 1, 2), T_1 (3, 4, 5) and T_2 (6, 7, 8). The WVs for all the triads were generated but the spatial distribution is presented only for T_{-2}, T_{-1}, T_0 and T_1 in Fig. 4(a). In T_{-2} *i.e.*, 4-6 days before normal NEM onset, winds are weak north of 16° N, well-organised SW winds prevail south of 14° N, save for S/SE winds close to north CTN and SCAP. ET which is not clearly defined during T_{-2} is markedly clear at 12° N in T_{-1}. The onset of firm easterlies and establishment of ET at 11° N is evident in T_0. During the onset triad T_0 the eastern end of the ET is located in a much more southerly latitude of nearly 8° N east of 88° E which is similar to the pattern of ET in pentad P_4 of Section 6.1.1. The movement of the ET further southward to 7° N after NEM onset is evident from T_1.

The diffused and transitional nature of easterly winds around 10 days before onset, the rapid southward movement of ET with the setting in of E / NE winds during onset phase and the prominent presence of easterlies north of ET are brought out with much more clarity in triad analysis than the pentad analysis of Section 6.1.1. Fig. 4(b) presents the distribution of scalar WS over BoB during the triads T_{-1} and T_0. The WS of 4-6 m/s off CTN and SCAP coast during T_{-1} increases sharply to 6-8 m/s during T_0. Over the region south of Comorin and Sri Lanka also, WS increases from T_{-1} to T_0. Spatially, WS decreases from west to east in T_0 *i.e.*, scalar WS increases as the wind blows from east to west at the time of onset. This striking feature is well brought out in T_0 and to a lesser extent in T_{-1}.

6.1.3. *Analysis of QS winds over BoB for the various phases of NEM activity over land*

By convention, the NEM season is accounted from 1 October to 31 December, though the DO and DW do not occur exactly on the beginning and end dates of the respective months. The pre-NEM onset days are from 1 October up to the day prior to DO. The NEM period between DO and DW (DW excluded) is considered as the duration of NEM which comprises the active and vigorous, light RF and dry (no RF) days of NEM. The days from DW to 31 December are classified as post-NEM withdrawal days even if the withdrawal took place in January of the succeeding year. Thus, five phases of NEM based on RF reported by land stations of CTN and SCAP have been classified which are pre-NEM (C_1),

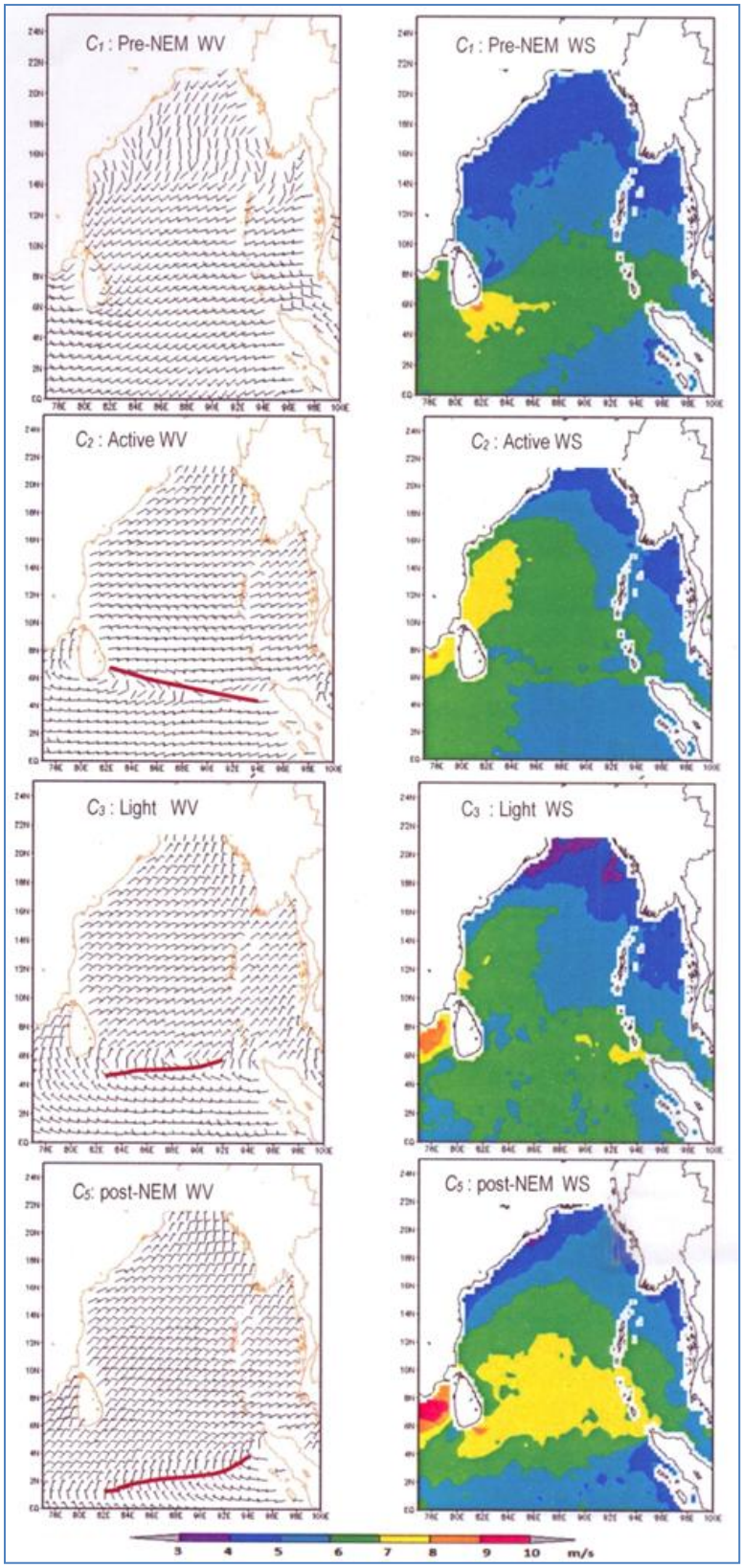

Fig. 5. QS mean OSW over BoB during phases of NEM, 1999-2008
(Dry phase not shown) WV - wind vector, WS - scalar wind speed (in m/s)

active and vigorous (C_2), light (C_3), dry (C_4) and post-NEM withdrawal (C_5). The IMD definitions in practice for classifying days based on strength and spatial distribution of RF during NEM and the grouping of days under three categories such as active, light and dry are provided in Table 2. During the NEM season of 1999-2008, BoB was affected by 30 CDs comprising of 116 days. The relatively strong winds during CD days and the various directions from which wind blows around the CD centre modify the surface wind pattern that would otherwise prevail on non-CD days. Hence, the 116 CD days have been excluded while identifying dates belonging to the categories C_1 to C_5.

The QS based WVs over BoB of days classified under C_1 to C_5 were derived for each category. The mean WV and scalar WS patterns thus generated are depicted in Fig. 5 save for C_4 (Dry) which is near identical to that of C_3 (Light). The mean scalar WS (m/s), its standard deviation (SD) and the frequency of the number of grid points for each of the five sectors of BoB for C_1 to C_5 phases of NEM were also computed and are presented in Table 3. The features that could be inferred from Fig. 5 and Table 3 are discussed below phasewise.

TABLE 2

Description of spatial distribution of DRF and strength of NEM

Classification of spatial distribution of DRF	Percentage of stations reporting DRF of at least 2.5 mm	
Dry (D)	Nil	
Isolated (I)	≤ 25	
Scattered (SC)	26 – 50	
Fairly Widespread (FW)	51 - 75	
Widespread (W)	≥ 76	
Strength of NEM	Ratio of DRF realised with reference to normal	Grouping of days of NEM season*
Vigorous	> 4, FW / W	Active
Active	> 1.5 – 4, FW / W	
Normal	0.5 – 1.5, SC	Light
Weak	≤ 0.5, I	
Dry	-	Dry

*****from date of onset (DO) to the date prior to date of withdrawal (DW)
DRF : Daily rainfall

(*i*) *Pre-NEM days (C_1)*

There were 130 C_1 days during the NEM season of 1999-2008. The spatial pattern of mean winds depicted in Fig. 5 is similar to that of pentad P_1 of October [Fig. 3(a)]. South of 14° N, weak SW winds prevail while southerlies are distinct over north BoB which turn to SW over head BoB. The mean scalar WS gradually increases from 4-5 m/s over head BoB to 6-7 m/s south of 10° N. Areas of scalar WS 7-8 m/s are observed both over Comorin and off south Sri Lankan coasts. Over the five sectors of BoB, the mean scalar WS (Table 3) is least over WC (4.8 m/s) and is 6.8 and 6.7 m/s over SSW and SSE BoB respectively.

(*ii*) *Active & vigorous days (C_2)*

There were 251 C_2 days. Winds which are NE / E over most parts of BoB become northerlies over GoM and Comorin areas of BoB that can be attributed to the topographical effect of land mass on both sides of GoM. ET is positioned around 5-6° N with SW (E) winds south (north) of ET. The scalar WS is strongest (7-8 m/s) in NSW BoB, parts of WC BoB and GoM and Comorin areas decreasing to 6-7 m/s over SSW and SSE BoB. South of the ET, WS is 5-6 m/s with the least scalar WS of 4-5 m/s over head BoB. Over the region of BoB north of 5°N, the scalar WS increases from east to west reaching the highest speed of 7-8 m/s off CTN and SCAP - a feature that is similar to T_0 as discussed in Section 6.1.2. Among the five sectors of BoB, NSW has a mean scalar WS of 7.2 m/s (Table 3) indicating that it is the most responsive sector for NEM over BoB when active NEM phase prevails over CTN. SSW and SSE BoB have almost equal mean scalar WS of 6.3 and 6.4 m/s (Table 3) respectively presumably due to southward shift of ET to 6° N.

(*iii*) *Light (C_3) and Dry (C_4)*

The spatial pattern is based on 70 C_3 days and 270 C_4 days (not shown as it is similar to C_3). NE winds prevail over BoB north of 5° N where ET is positioned. Weak SW winds prevail south of ET. Stronger (weaker) northerlies are observed over GoM and Comorin areas (head BoB) compared to active NEM days. Mean scalar WS south of 8° N and east of 80° E is predominantly 6-7 m/s and the highest WS (8-9 m/s) is over Comorin area of BoB. During C_3 sectorwise mean scalar WS is 6.7 m/s over SSE, NSW BoB while it is least in NSE at 5.9 m/s (Table 3). During C_4 the ET was well-marked in the eastern longitudes where it is oriented along 6° N.

(*iv*) *Post-NEM (C_5)*

There were 83 C_5 days. NE winds are observed over most of BoB which are stronger south of 14° N and over GoM and Comorin. Weak northerlies are observed over head BoB. The ET is located along 1-3° N but shifts to

TABLE 3

QS mean scalar OSW speed (in m/s) over the five sectors of BoB during the phases of NEM

Phase of NEM	Sector of BoB					Range of SD (m/s)	Number of days
	WC	NSW	NSE	SSW	SSE		
C_1	4.8	5.3	6.0	6.8	6.7	2.8 - 3.4	130
C_2	6.8	7.2	6.5	6.4	6.3	2.5 - 2.9	251
C_3	6.0	6.7	5.9	6.3	6.7	2.6 - 3.0	70
C_4	6.1	6.9	6.6	6.6	6.2	2.4 - 3.0	270
C_5	5.8	7.0	7.2	7.4	7.5	1.6 - 2.5	83
Range of *n*	664 - 666	418 - 423	496 - 500	357 - 360	532 - 535		

Period of study : 1 Oct - 31 Dec, 1999-2008, excluding days of cyclonic disturbances (CDs)

QS : QuikSCAT, OSW : Ocean Surface Wind, BoB : Bay of Bengal, NEM : North East Monsoon

WC, NSW, NSE, SSW and SSE : As in Fig. 1

n : Number of grid points, SD : Standard Deviation

C_1: Pre-NEM, C_2 : Active, C_3 : Light, C_4 : Dry, C_5 : Post-NEM withdrawal days

m/s : metre per second, 1 m/s = 1.944 knots

TABLE 4

QS mean scalar OSW speed (in m/s) over the five sectors of BoB during OLR episodes of NEM

OLR criterion*	Sector of BoB					Range of SD	Mean **	Number of days	Range of *n*
	WC	NSW	NSE	SSW	SSE				
O_1	8.1	8.4	7.6	7.7	7.2	2.8 - 3.3	7.8	46	355 - 664
O_2	6.3	6.9	6.5	6.6	6.7	2.4 - 3.2	6.6	180	358 - 664
O_3	6.0	6.9	6.5	6.7	6.7	2.0 - 2.8	6.5	98	357 - 664
O_4	5.9	6.6	6.4	6.2	6.2	2.0 - 2.2	6.2	246	359 - 664

Period of study : Date of onset up to 31 Dec, excluding CD days, 1999-2008

QS, OSW : Ocean Surface Wind, BoB, NEM, *n*, SD, CD: As in Table 3

WC, NSW, NSE, SSW and SSE : As in Fig. 1, OLR : Outgoing Longwave Radiation

O_1: OLR≤200; O_2 : 200 - 230 ; O_3 : 230 - 240; O_4 : >240 Wm^{-2}

Over the five sectors of BoB : *Mean OLR computed, **** :** Weighted mean scalar wind speed (in m/s)

higher latitudes over the eastern longitudes (80-96° E). The scalar WS at 9-10 m/s over Comorin area is strongest when compared to those of the rest of the phases of NEM in the same area. The sectors SSW and SSE BoB report the highest mean scalar WS (7.5 m/s), apparently due to prevalence of active NEM phase over Sri Lanka & adjoining BoB during the post-NEM withdrawal phase over CTN. The SD of the mean scalar WS during C_1-C_5 days for the five sectors presented in Table 3 ranges from 1.6 to 3.4 m/s. However, 60% of the SDs were higher than 2.4 m/s indicating the substantial variability in mean winds.

Some of the normal salient aspects of the above analysis of QS winds during the phases of NEM are highlighted below:

(*i*) Position of ET which is around 6° N in C_2 settles around 2-3° N during C_5.

(*ii*) WS is highest in C_2 over NSW which is the best representative sector of BoB for NEM activity over land.

(*iii*) During all the phases of NEM season, northerly winds prevail over GoM and Comorin areas of BoB

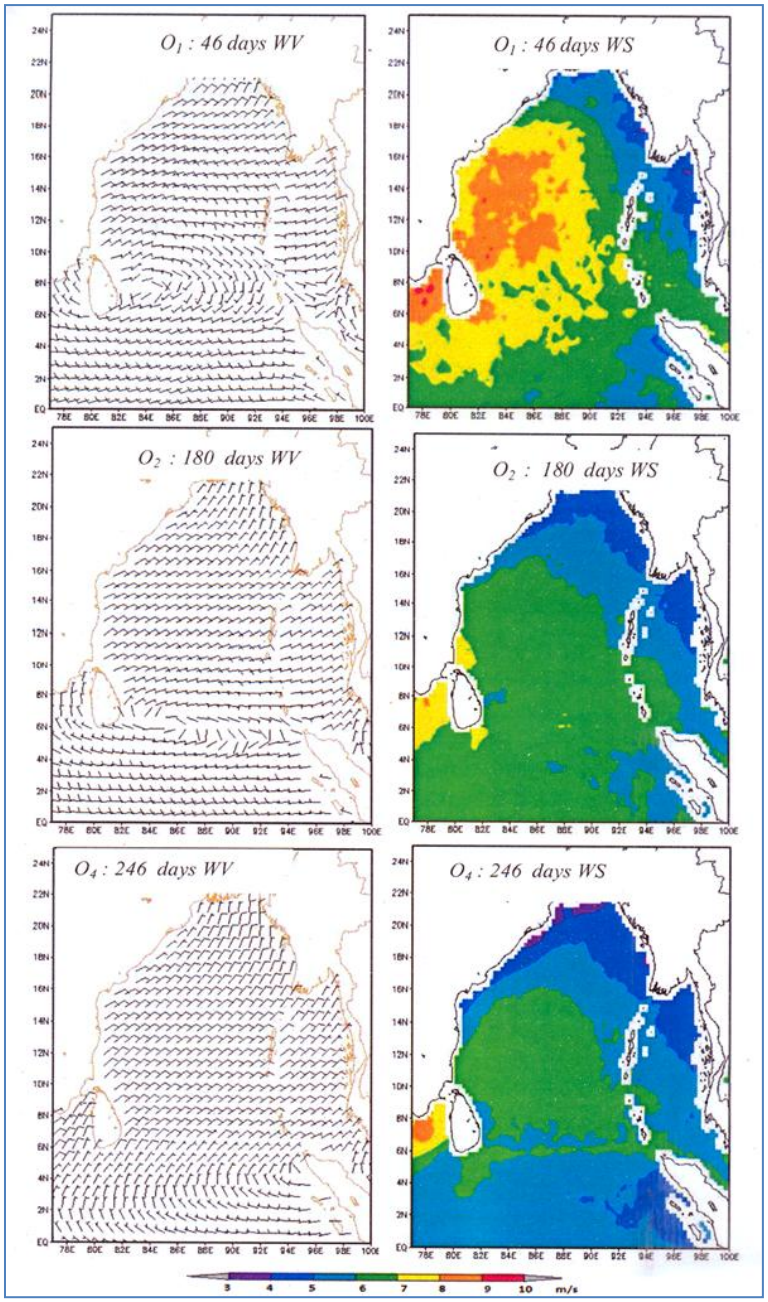

Fig. 6. QS mean OSW over BoB during OLR episodes of NEM, 1999-2008
O_3 pattern not shown. WV – wind vector, WS – scalar wind speed (in m/s)

apparently due to the topographical effect of the land mass on either side of GoM.

(*iv*) Scalar WS remains higher over GoM and Comorin areas throughout C_2 to C_5 compared to the rest of BoB, reaching 8-9 m/s during C_5.

(*v*) Despite RF activity being entirely different during C_2 and C_4 days, almost similar pattern of distribution of WS is observed in the sectors of BoB except for WC which has higher WS in C_2 than C_4 days.

(*vi*) WS is stronger during C_4 compared to C_3 days, though the flow pattern of winds is almost identical.

(*vii*) During C_5 days, higher WS is observed over SSW, NSE and SSE compared to C_1 to C_4 and the prominent

TABLE 5

Buoy mean OSW during the phases of NEM

Phase of NEM	Identifier of the buoy and sector of BoB																					
	DS05 WC			OB10 WC			SW06 WC			AN04 NSE*			OB08 NSW			DS03 NSE			AN05 NSE*			SW05 GoM			OT01 GoM		
	WV : ddd ff WS																										
C_1	287	01	3.7	179	01	3.5	172	00	3.5	121	01	2.9	227	02	3.9	226	03	4.4	238	05	5.6	206	03	4.9	279	03	5.5
C_2	049	03	5.6	058	05	5.8	036	04	5.1	083	03	4.5	052	03	5.7	057	04	5.1	057	04	4.1	017	04	5.4	072	04	5.8
C_3	012	02	4.2			0.0	037	05	5.5			0.0	038	04	4.9	059	05	5.2			0.0	025	07	7.3	022	07	7.2
C_4	018	02	5.5	027	03	5.1	036	05	5.9	081	01	3.5	050	07	5.5	050	04	5.7	038	05	5.2	023	05	7.1	067	05	6.1
C_5	031	04	5.2	036	05	4.9	027	05	5.6	082	02	6.2	026	06	5.9	044	04	5.8	047	05	6.3	028	07	7.7	072	07	6.9
Total number of observations (C_1 to C_5)	3647			567			1980			526			2006			3062			792			2272			1050		
Range of SD of mean scalar WS	2.0 – 2.5			1.8 – 2.3			1.7 – 2.0			1.8 – 2.8			1.9 – 2.7			1.7 – 2.7			1.4 – 2.9			1.5 – 2.5			1.8 – 2.9		
Availability of data during Oct-Dec (1999-2008)	OND(2000, 02, 04-07), O-03			OND2008			O (2000,02, 04), partial O-01, OND(03, 06)			OND 2005, N-06			OND (2003,05,07), D-02			OND (1999, 00,02-03), ON-04, 17-31D-05, O-07			20-31D-05, OND-06			OND(1999, 00,01,06), O-02, 1-16N-02, 1-17 O-05			ON 2000, OND-02, 1-18O-03		

Period of study : Oct –Dec, 1999-2008 excluding days of CDs, QS, NEM, BoB, C_1 to C_5, SD, CD : As in Table 3

WC, NSE, NSW : As in Fig.1, * : Close to, GoM : Gulf of Mannar

WV : Wind vector, ddd : Wind direction (degrees), ff (given here in m/s) : Wind speed,

WS : Mean scalar wind speed (in m/s), O, N, D : As in Table 1.

region of high WS lies over the central longitudes of BoB between 4 and 10° N.

(*viii*) During C_2 days, WS increases from east to west while during C_4 days WS decreases from south to north.

6.1.4. *Analysis of QuikSCAT winds during various phases of convective activity over BoB*

In this section, the mean OSW over BoB based on QS for different categories of NEM activity over the ocean are analysed. Conventional RF data is not available over the sea but satellite-derived OLR which is an index of convection could be taken as a proxy indicator for RF over the oceans as explained in Section 5. The OLR criteria O_1 to O_4 have already been defined. Using the daily temporal mean OLR data described in Section 4.4, the daily mean OLR was computed for the days of the study period 1 October-31 December, 1999-2008 for each of the five sectors of BoB *viz*., WC, NSW, SSW, NSE and SSE.

For the resolution (0.25° × 0.25°) of the QS pass data, the number of grid points at which data must ideally be available over the sectors WC, NSW, NSE, SSW and SSE are 864, 572, 660, 572 and 660 respectively. However, actual data available is less due to the variation in the swath area for each pass and the quality control procedures adopted. A mean value of the number of grid points for each sector over which data is available was computed and the weighted mean of OLR over the five sectors of BoB was derived for each day of the NEM season for the 10 year period 1999-2008. The resultant OLR values and the days corresponding to the four OLR categories O_1, O_2, O_3 and O_4 with frequencies 46, 180, 98 and 246 days respectively were grouped together. The mean scalar WS for the five sectors of BoB during O_1 to O_4 are provided in Table 4. The number of days, SD of WS and the range of the number of grid points are also given as supplemental information. The QS derived spatial mean WV and scalar WS patterns over BoB for all the four categories were generated and only those of O_1, O_2 and O_4 are presented in Fig. 6.

The inferences drawn from a critical analysis of Fig. 6 and Table 4 are discussed below:

(*i*) O_1 : There were 46 O_1 (OLR ≤ 200 Wm^{-2}) days. NE winds prevalent over head BoB turn to easterlies between 12 and 14° N. ET is around 7°N with SW winds blowing

south of ET. NW winds are observed in GoM and Comorin areas with highest mean scalar WS of 9-10 m/s in few pockets. Strengthening of WS (8-9 m/s) in sectors of BoB close to CTN and SCAP of SPI which gradually decrease to 5-6 m/s over head BoB is evident. Similar to the active (C_2) phase of NEM, scalar WS increases from east to west over most parts of BoB. As seen from Table 4, the mean scalar WS (m/s) is highest at 8.4 (lowest at 7.2) in NSW (SSE) sector implying again that NSW is the preferred and representative sector of NEM activity over BoB.

(*ii*) O_2 and O_3 : WV and WS patterns derived from 180 O_2 and 98 O_3 days (not shown in Fig. 6) are almost identical. NE winds and scalar WS of 6-7 m/s prevail over most parts of BoB. However, in GoM and Comorin areas, weak northerlies prevail in O_2 which become NNE in O_3 days while scalar WS is higher (8-9 m/s) in O_3 than in O_2. ET is positioned at 6 (5)° N in O_2 (O_3) days. Similar to C_4 (dry days) scalar WS increases from north to south over most parts of BoB. The mean scalar WS values provided in Table 4 are almost the same in the four sectors during O_2 and O_3 (6.5-6.9 m/s) days except over WC where it is slightly higher in O_2 (6.3) than O_3 (6.0).

(*iii*) O_4 : WV and WS patterns are derived from 246 O_4 days. Northerlies over head BoB turn to NE winds immediately southwards. The ET is positioned at 4° N with westerly winds prevailing further south. The scalar WS is predominantly 6-7 m/s over the five sectors of BoB decreasing to 5-6 m/s south (north) of 5 (16)° N. The lowest WS is 4-5 m/s over head BoB. Scalar WS over Comorin (GoM) area is 6-9 (7-8) m/s. Both the vector and scalar WS are higher in these two areas. Similar to O_2 and O_3 scalar WS by and large increases from north to south.

From Table 4, it is seen that WC has lesser mean scalar WS (5.9 m/s) compared to the other four sectors with NSW experiencing the highest WS (6.6 m/s). The SD of mean scalar WS in the five sectors of BoB ranges from 2.0-3.3 m/s for O_1 to O_4. The weighted means of the scalar WS of the five sectors are 7.8, 6.6, 6.5 and 6.2 respectively for O_1, O_2, O_3, O_4 days exhibiting a near-linear decrease signifying the close relationship sector-to-sector between scalar WS and convection.

Salient features of the analysis based on OLR criteria O_1 to O_4 are:

(*i*) During O_1, easterlies prevail over the five sectors and the central parts of BoB which become NE in O_2 and O_3 with more of a northerly component in O_4 days.

(*ii*) The southward shift in ET from 8° N (O_1), 6-7° N (O_2), 5° N (O_3) to 1-3° N (O_4) is prominent.

(*iii*) O_1 days have the highest mean scalar WS (7-8 m/s) in sectors of BoB close to CTN, SCAP, GoM and Comorin areas denoting the strengthening phase of NEM activity over BoB.

(*iv*) The mean scalar WS increases from east to west during O_1 days while it decreases from south to north during O_2-O_4 days analogical to T_0 of Fig. 4 and C_2 of Fig. 5.

(*v*) Mean scalar WS is highest (lowest) in O_1 (O_4) days at 7.8 (6.2) m/s with intermediate and near identical values for O_2 (6.6) and O_3 (6.5) for all the five sectors of BoB.

(*vi*) NSW has the highest mean scalar WS during O_1 to O_4 days, signifying that it is the most representative feeder sector over BoB for NEM activity over land.

(*vii*) The SD over the five sectors of BoB ranges from 2 to 3.3 m/s.

(*viii*) GoM and Comorin areas of BoB have highest WS of 8-9 m/s during O_1, O_3 and O_4 days with slightly lesser WS (7-8 m/s) in O_2 days.

6.2. *Analysis based on buoy data*

6.2.1. *Features of OSW from buoy data*

The mean OSW reported by buoys during the phases of NEM activity *viz*., C_1 to C_5 was derived to effect comparison between both QS and buoy based OSW at point locations. CD days were first excluded and then the remaining days for which buoy data was available under C_1 to C_5 were grouped together. An analysis similar to that of Section 6.1.3 was then conducted. The mean WV, mean scalar WS and its SD have been computed for C_1 to C_5 categories for the 9 buoys and results are presented in Table 5. As such there is wide dispersion in the periods of data availability for the 9 buoys. Each buoy has transmitted several observations per day and hence the total number of observations ranged from 567-3647, making the mean wind parameters reliable. The buoy derived mean winds at the respective coordinates were visually compared with the corresponding QS based spatial pattern of mean winds provided in Fig. 5 for the phases of NEM.

Salient features of the analysis are presented below:

(*i*) In pre-NEM (C_1) days, near southerly winds are reported by the two buoys OB10 and SW06 in WC (Table 5). AN04 located close to the NE corner of NSE BoB has reported SE winds consistent with the QS winds in its neighbourhood which are also SE. Mean WV of

other buoys in BoB south of 14° N is SW. By and large, buoy based winds are in conformity with the QS derived winds as in Fig. 5 for C_1. The mean scalar WS computed from buoy data ranges from 2.9 to 5.6 m/s.

(*ii*) In active and vigorous (C_2) to post-NEM (C_5) days, all the buoys have reported NE mean WV conforming to Fig. 5. The mean scalar WS from buoys ranged from 4.1-5.8 m/s in C_2 days while QS winds ranged from 6.3-7.2 m/s over the sectors of BoB. During C_3 days, SW05 and OT01 reported 7.2-7.3 m/s which conforms to the higher scalar WS pattern observed over GoM and Comorin areas. In C_4 and C_5 days, higher mean scalar WS is reported by buoy SW05 in GoM area in conformity with Fig. 5. The SD of WS up to 2.9 m/s indicates the large extent of WS variability.

(*iii*) For buoy SW05 located in the GoM, the winds are predominantly northerlies during C_2 to C_5 phases, consistent with the mean winds generated from QS analysis.

(*iv*) For all the 9 buoys, WS during C_1 is lower than that of the other phases. Buoys in and close to NSE, NSW sectors of BoB and GoM reported higher WS in the post-NEM phase than those in WC. By and large, WS is not the highest when NEM is active over CTN.

The above inferences are position-specific as the buoy locations are neither representative of the five sectors of BoB considered nor is the data availability consistent. However, comparison with QS winds at the locations of buoys can be made as the former is available at most of the grid points. Such an analysis based on direct comparison yielded the general inference that the QS WS is higher than the buoy WS by 10-15%.

6.2.2. *Reduction of wind speed in surface layer*

As stated in Section 3.1, the OSW from QS are referenced to a height of 10 m whereas buoy based winds are reported from 3 m above m.s.l. It is well known that wind at the lowest levels of the atmosphere varies with height due mainly to friction. Therefore in order to effect a comparison between QS and buoy based OSW, the WS at 10 m, given that at 3 m has to be determined or vice versa. Such a task could be accomplished by resorting to the theoretical profiles of variability of winds in the lowest vertical layer. The logarithmic wind law for the lowest turbulent layer [Kara *et al.* (2008)] of the planetary boundary layer can be applied to determine the varying profile of vertical winds under neutrally stratified conditions of atmospheric stability.

The WS $\bar{u}$ at a vertical height z [Hess (1959)] is given by:

$$\bar{u} = \frac{u_*}{k}\ln\left(\frac{z}{z_0}\right)$$

$$\bar{u}_3 = \frac{u_*}{k}\ln\left(\frac{z_3}{z_0}\right)$$

$$\bar{u}_{10} = \frac{u_*}{k}\ln\left(\frac{z_{10}}{z_0}\right)$$

$$\frac{\bar{u}_3}{\bar{u}_{10}} = \frac{\ln\left(\frac{z_3}{z_0}\right)}{\ln\left(\frac{z_{10}}{z_0}\right)}$$

where, u_* is the friction velocity, $\bar{u}_{10}$ and $\bar{u}_3$ denote the WS at heights z_{10} = 10 m and z_3 = 3 m, k is the von Kármán constant and z_0 is the roughness parameter. The typical value of k ranges from 0.38 to 0.4 and z_0 for oceans is 1.52×10^{-4} m (Peixoto and Oort, 1992). Incorporating these values in the formula, we obtain $\frac{\bar{u}_3}{\bar{u}_{10}} = 0.89$ and $\frac{\bar{u}_{10}}{\bar{u}_3} = 1.12$.

In other words, $\bar{u}_3$ is 11% lower than $\bar{u}_{10}$ and $\bar{u}_{10}$ is 12% higher than $\bar{u}_3$. Considering the result reported in Section 6.2.1 that QS WS derived in the study is 10-15% higher than buoy based OSW speed, it is evident from the aforesaid analysis that the QS OSW speeds are comparable to buoy OSW if the former is brought to the level of the latter or *vice versa*.

7. Discussions

In the preceding sections, results of the analysis performed utilising QS based surface winds over BoB during NEM season were presented. The southward movement of ET over Indian peninsula during October-November-December especially in October is a remarkable meteorological event which has been well documented based on surface pressure and lower tropospheric wind data [Raj and Jamadar (1990) and Raj *et al.* (loc.cit.)]. The present study on the Indian NEM based on QS OSW is the first of its kind in the systematic documentation of ET over BoB during OND and the results are consistent with those of the former. The ET over BoB moves from south to north but the dip of the ET to a lower latitude of 8° N during P_4 and T_o is consistent with the formation of clouds over a southerly latitude and their movement towards SPI during the onset phase. This pattern is consistent with the thematic model of NEM onset advanced by Raj *et al*. (loc.cit).

The scalar WS over BoB increases from north to south for most of the episodes but it is significant that it

increases from east to west reaching maximum speed of 8-9 m/s off CTN and SCAP during the episodes of onset, C_2 and O_1. During such instances, the origin of air parcels which hit CTN / SCAP coast can be traced to eastern parts of BoB. As the WS increases substantially during the movement of the air parcels from eastern BoB to SPI coast, there is velocity divergence off the coast and frictional convergence at the coast. This dynamical feature is consistent with the RF climatology of the coast receiving slightly, *i.e*., around 10% more RF than the adjacent ocean areas. Such a climatological feature has been derived based on satellite and DWR data [Suresh and Raj (2001); Raj (2012); Amudha *et al.* (2016b&c)]. The presence of high WS over most of the sectors during the post-NEM (C_5) period over SPI is evident from Table 3. Apart from continued NEM activity over the Sri Lankan region, another factor that could be responsible for the strong winds is the increase in surface pressure over the northern latitudes of India as the winter season advances. In a broader sense, such a feature could be attributed to intense outflow from the Siberian High as well. The GoM and Comorin areas of BoB display a unique signature with northerly winds during C_2 and higher scalar WS prevailing throughout C_1 to C_5 compared to the rest of BoB. Even when dry NEM (C_4) conditions prevail over land, WS reaches 9-10 m/s in this area. The WS data from moored buoys SW05 and OT01 deployed in GoM and Comorin areas also support the fact that these areas experience relatively higher WS compared to other sectors.

QS mapping of OSW is essentially based on geophysical model function algorithm. Complex regression equations with suitable weightage factors for multiple atmospheric / oceanic parameters form part of the computations. Technological advancements have facilitated the design upgradation and improvement of software used in remote mapping of OSW so as to overcome inherent limitations like contamination/noise in measurements during heavy rain. ASCAT scatterometer, launched by EUMETSAT and operational since 2007 has improved algorithms and once the database generated is sufficiently long, will serve well for further studies on OSW over BoB during all the seasons including the NEM season. The SCATSAT-1 launched by Indian Space Research Organisation on 26 September, 2016 provides OSW at high resolution and can be potentially useful for analysis of winds over the NIO.

8. Conclusions

The results of the study are presented below:

(*i*) The spatial variability of the mean WV and scalar WS of OSW over BoB during NEM season was generated and analysed for 18 pentads / hexads of the period 1 October-31 December. Over north BoB in October, winds which are SW during P_1 and P_2 become NE by P_3 just prior to the onset of NEM. ET which is diffuse in P_3 is firmly established along 14° N by P_4 at the time of onset of NEM and gradually shifts to around 2-3° N by December. By H_{18} ET is located around 1.5° N.

(*ii*) Triad compositing of winds by superposed epoch analysis brought out the diffused and transitional nature of easterly winds prior to onset and the southward movement of ET after onset, with better clarity than pentad analysis.

(*iii*) Spatial patterns of WV and scalar WS generated for the five phases of NEM C_1 to C_5 *viz*., pre-NEM, active, light, dry and post-NEM withdrawal indicated that the ET whose position is around 6° N in C_2 settles around 2- 3° N in C_5.

(*iv*) During C_2, easterlies prevail over most parts of BoB. NSW sector of BoB has the highest mean scalar WS ranging from 7 to 8 m/s. This sector is the most representative feeder sector with a mean WS value of 7.2 m/s when active NEM conditions prevail over SPI.

(*v*) The scalar WS pattern is almost the same in most sectors of BoB except WC during C_2 and C_4 days despite the distinct contrast in RF activity over CTN during such days. Higher WS prevail over BoB off SPI during C_2 days with WS increasing from east to west while during C_4, the decrease of WS is from south to north.

(*vi*) Throughout C_2 to C_5 WS of 8-9 m/s prevailed over Gulf of Mannar and Comorin areas of BoB. Northerly winds prevailed over these areas during the NEM season apparently due to topographic effect of the land mass lying on either side of GoM.

(*vii*) Analysis based on OLR criteria for convective activity over BoB revealed the southward shift of ET from 8° N (O_1) to 1-3° N (O_4) similar to C_1 to C_5.

(*viii*) During O_1 days, the mean scalar WS over BoB increases from east (4-5 m/s) to west (8-9 m/s). In the case of O_2-O_4 days, WS decreases from south to north (6-7 m/s to 4-5 m/s) save for GoM and Comorin areas.

(*ix*) The mean scalar WS over BoB are higher (8-9 m/s) in O_1 days and lower (6-7 m/s) during O_4 days. GoM and Comorin areas reported highest WS of 8-9 m/s on O_4 days.

(*x*) During O_1 days, the highest mean scalar WS is 8.4 m/s over NSW BoB and lowest of 6.2 m/s is over SSW and SSE sectors on O_4 days.

(*xi*) The theoretical profile of variability in vertical winds over BoB has revealed that the winds at 3 m reference height will be lower by 11% than winds at 10 m. WS reported by both QS and buoy brought to the same level are well comparable and have good consistency.

Acknowledgement

The authors thank the Deputy Director General of Meteorology, Regional Meteorological Centre, Chennai for the facilities provided during the study. The authors acknowledge INCOIS, Hyderabad for supplying the data from moored buoys deployed by NIOT, Chennai. The help rendered by S/Shri M. Bharathiar and N. Selvam, Scientific Assistants, RMC Chennai in preparing few of the figures is also acknowledged.

Disclaimer : The views expressed in this research paper are those of the authors' and do not necessarily reflect the views of the organisation to which they are affiliated.

References

Agarwal, N., Sharma, R., Basu, S. K. Sarkar, A. and Agarwal, V. K., 2007, "Evaluation of relative performance of QuikSCAT and NCEP reanalysis winds through simulations by an OGCM", *Deep Sea Res. I: Oceanogr. Res. Pap.*, **54**, 1311-1328.

Amudha, B., Raj, Y. E. A. and Asokan, R., 2016a, "Characteristics of movement of low level clouds associated with onset / wet spells of northeast monsoon of Indian sub-continent as derived from high resolution INSAT OLR data", *Mausam*, **67**, 2, 357-376.

Amudha, B., Raj, Y. E. A. and Asokan, R., 2016b, "Spatial variation of clouding / rainfall over southeast Indian peninsula and adjoining Bay of Bengal associated with active and dry spells of northeast monsoon as derived from INSAT OLR data", *Mausam*, **67**, 3, 559-570.

Amudha, B., Raj, Y. E. A., Asokan, R. and Thampi, S. B., 2016c, "Spatial rainfall patterns associated with Indian northeast monsoon derived from high resolution rainfall estimates of Chennai DWR", *Mausam*, **67**, 4, 767-788.

Geetha, B., 2011, Ph.D. thesis, "Indian northeast monsoon as a component of Asian winter monsoon and its relationship with large scale global and regional circulation features", University of Madras, Chennai.

Geetha, B. and Raj, Y. E. A., 2015, "A 140-year data archive of dates of onset and withdrawal of northeast monsoon over coastal Tamil Nadu: 1871-2010 (Re-determination of 1901-2000), *Mausam*, **66**, 1, 7-18.

Hess, L. Seymour., 1959, "Introduction to Theoretical Meteorology", Henry Holt and Company, New York, 276-279.

India Meteorological Department, 2003, Cyclone Manual, O/o Dy.Director General of Meteorology (Weather Forecasting), Pune.

India Meteorological Department, 2008, Forecasters' Guide, O/o Dy. Director General of Meteorology (Weather Forecasting), Pune, p77.

Kara, A. B., Wallcraft, A. J. and Boourassa, M. A., 2008, "Air-sea stability effects on the 10 m winds over the global ocean: Evaluations of air-sea flux algorithms", *J. Geophys. Res.*, **113**, C04009, doi: 10.1029/2007JC004324.

Liu, W. T. and Tang. W., 1996, "Equivalent neutral wind", JPL Publication 96-17, NASA, California.

Liu, W. T., 2002, "Progress in scatterometer application", *J. Oceanogr*., **58**, 121-136.

Loe, B. R., Verma, B. L., Giri R. K., Bali S. and Meena L. R., 2006, "Recent very severe tropical cyclones over the Bay of Bengal: Analysis with satellite data", *Mausam*, **57**, 1, 37-46.

Panofsky, H. A. and Brier, G. W., 1968, "Some applications of statistics to Meteorology", University Press, Pennsylvania, 80-104.

Peixoto, J. P. and Oort, A. H, 1992, Physics of Climate, *Am. Inst. of Phys*., Woodbury, New York, p520.

Physical Oceanography DAAC, Sea winds on QuikSCAT level 3 daily, gridded ocean wind vectors (JPL sea winds project), 2001, Guide document, Version 1.1., Jet Propulsion Laboratory, California Institute of Technology, D-20335.

QuikSCAT science data product - user's manual, 2006, Overview and geophysical data products, Jet Propulsion Laboratory, California Institute of Technology, Version 3.0, D-18053-Rev A.

Raj, Y. E. A. and Jamadar, S. M., 1990, "Normal dates of onset and withdrawal of southwest and northeast monsoons over the southern peninsula", *Vayumandal*, July-Dec, 76-84.

Raj Y. E. A., 1992, "Objective determination of northeast monsoon onset dates over coastal Tamil Nadu for the period 1901-90", *Mausam*, **43**, 3, 272-282.

Raj, Y. E. A., 2003, "Onset, withdrawal and intra-seasonal variation of northeast monsoon over coastal Tamil Nadu, 1901-2000", *Mausam*, **54**, 3, 605-614.

Raj, Y. E. A., Asokan, R. and Revikumar, P. V., 2007, "Contrasting movement of wind based equatorial trough and equatorial cloud zone over Indian southern peninsula and adjoining Bay of Bengal during the onset phase of northeast monsoon", *Mausam*, **58**, 1, 33-48.

Raj, Y. E. A., 2012, Monsoon Monograph, Vol. I, India Meteorological Department, Pune, Ch. 13, 606-670.

Sarkar A., 2003, "Space based techniques for remote sensing of oceanic winds - A review", *Mausam*, **54**, 111-120.

Satheesan, K., Sarkar, A., Parekh, A., Ramesh Kumar, M. R. and Kuroda, Y., 2007, "Comparison of wind data from QuikSCAT and buoys in the Indian Ocean", *Int. J.Remote Sensing*, **28**, 2375-2382, doi.10.1080/01431160701236803.

Singh, O. P. and Singh H., 2011, "Use of scatterometer based surface vorticity fields in forecasting genesis of tropical cyclones over the north Indian Ocean", *Mausam*, **62**, 1, 61-72.

Suresh, R. and Raj, Y. E. A., 2001, "Some aspects of Indian northeast monsoon as derived from TOVS data", *Mausam*, **52**, 4, 727-732.

Venkatesan, R., Shamji, V. R., Latha, G., Simi Mathew, Rao, R. R., Arul Muthiah and Atmanand, M. A., 2013, "*In situ* ocean subsurface time series measurements from OMNI buoy network in the Bay of Bengal", *Curr. Sci.*, **104**, 1166-1177.

Wenqing Tang, W. Timothy Liu and Bryan W. Stiles, 2004, "Evaluation of High-Resolution Ocean Surface Vector Winds Measured by QuikSCAT Scatterometer in Coastal Regions", *IEEE transactions on Geoscience and Remote Sensing*, **42**, 8, 1762-1769.